23rd ABCM International Congress of Mechanical Engineering
December 6-11, 2015, Rio de Janeiro, RJ, Brazil

CFD ANALYSIS OF THE CO-COMBUSTION PROCESS OF COAL AND WOODY BIOMASS: PARTICLE SIZE INFLUENCE

Cristiano V. da Silva[1], Leandro L. Felipetto, Ademir J. Velicko, Mateus J. Kominkiewicz and Arthur B. Beskow
Depart. of Mechanical Engineering - Universidade Regional Integrada do Alto Uruguai e das Missões - URI, Erechim, RS, Brazil.
1- cristiano@uricer.edu.br

Fernando M. Pereira
Department of Mechanical Engineering – Federal University of Rio Grande do Sul - UFRGS, Porto Alegre, RS, Brazil.
fernando@mecanica.ufrgs.br

Maria L. S. Indrusiak
Graduate Program in Mechanical Engineering – University of Vale do Rio dos Sinos – UNISINOS, São Leopoldo, RS, Brazil.
mlsperb@unisinos.br

Abstract. *This study aims at assessing through modeling and CFD simulations (Computational Fluid Dynamics) the behavior of the co-combustion of coal and biomass in a thermal power plant designed for coal as fuel. The simulations are conducted in 1:1 scale. In this context, the influence of the biomass particles size on the burning efficiency and on the pollutant and CO_2 emissions were evaluated. Velocity, temperature, pressure and concentration fields inside the boiler were numerically determined using the commercial software Ansys CFX 15.0. Numerical simulations were carried out for six different sizes for the biomass particles and all cases were then compared with a base case using only coal. It is considered for the six cases that the biomass in the mixture has the proportion of 1.74% of the mass flow of fuel, with 6% moisture by weight. For coal, it is considered a moisture of 16.47% in mass, and a parametric distribution of particle size. The main result observed was a reduction in emissions of CO and CO_2, from the implementation of co-combustion of coal with biomass. One can also observe a boiler temperature rise directly proportional to the increase in diameter of the biomass particles, and for Case 3 (300 μm), the temperature profile inside the boiler is similar to that shown when only coal is used as fuel.*

Keywords: *coal, wood, particle size, co-firing, CFD.*

1. INTRODUCTION

Coal is the main fossil fuel available and is responsible for approximately 27% of commercial production of world primary energy. Approximately 34% of all electricity generated in the world comes from the pulverized coal combustion (Williams et al., 2001). However, this method of electricity generation presents high rates of air pollutant emissions, such as carbon monoxide and dioxide (CO and CO_2), and nitrogen and sulfur oxides (NO_x and SO_x). The increase of thermal power plants efficiency worldwide would result in a significant reduction of CO_2 emissions and increase the lifetime of coal reserves. In addiction, the conversion of coal power plants to co-firing with biomass would have an even greater effect on reducing emissions of greenhouse gases, with a low investment (Dong et al., 2010), also resulting in longer life of coal reserves (Williams et al., 2001).

Co-combustion of pulverized coal with biomass in thermal power plants has been advocated for years considering its economic and environmental advantages. This is mainly due to reduced emissions of pollutants such as CO_2, or avoided emissions when replacing part of the coal for biomass, which has zero net emission of carbon dioxide. For this reason its use is gradually increasing. Currently, in the UK, a substantial amount of electricity is generated by this way in large thermal power plants that have adopted the addition of small amounts of biomass, around 2-4% in thermal base. (Backreedy et al., 2005). Currently, there are many studies on coal-biomass combustion in the literature.

Wurzenberger et al. (2002) showed a transient model of a single particle in bed combustion. First, pyrolysis has been described by independent parallel reactions. Then cracking of tar, homogeneous reactions of gas and heterogeneous reactions of char were described. The validation of the particulate combustion model was performed using experimental data on spherical particles of beech wood. In another study, Porteiro et al. (2006) reported the use of a mathematical model which describes the thermal conversion of biomass particles. Biomass pyrolysis was modeled using three concurrent reactions that produce light gas, tar and char. In their work the following additional kinetics were considered: char combustion producing carbon monoxide and carbon dioxide and combustion of hydrogen on the particle surface (cylindrical briquettes). The validation was done using a mass loss model. In another study, Backreedy et al. (2006) showed chemical models applicable to the study of coal combustion processes. Modeling of NOx formation is characterized as a three-way process, which is typically simplified as NO-fuel, NO thermal and NO-prompt. Ma et al. (2007) developed a CFD model for pulverized coal-biomass combustion in a boiler and presented results for the combustion of wood in a typical installation of industrial tests of 1 MW. The model is essentially based on sub-models

for coal combustion using an Eulerian-Lagrangian framework. Numerical predictions were compared with some experimental measurements and a good agreement was reached.

The particle combustion model presented by Lu et al. (2008) considers drying, devolatization, gasification and char oxidation and combustion. The Shafizadeh and Chin (1977) kinetic scheme for the decomposition of biomass was used, assuming the biomass decomposition into light gases, tar and char by three parallel reactions. Tar is submitted to subsequent reactions producing char and volatile gases. Heterogeneous reactions were modeled by accounting for gasification and oxidation of char with water vapor and carbon dioxide. Gaseous reactions considered were the gas phase oxidation of hydrogen, carbon monoxide and a cluster of hydrocarbons represented by the empirical formula C_6H_6,$2O_{0,2}$. Validation of the model was made by comparison with experimental data. Yang et al. (2008) conducted a two-dimensional simulation on a single cylindrical wood particle. The sub-processes studied were very similar to those used by Lu et al. (2008), but different schemes were implemented to achieve the particle conversion chemistry.

Yin et al. (2010) presented a model for co-combustion of coal-wheat straw in a 150 kW stabilized spiral reactor with dual feeding. The model allowed for the prediction of mass, temperature, density and particle size variation along their routes. On the same line, Gil et al. (2010) studied the co-combustion of Pinnus sawdust in a non-isothermal thermogravimetric method. Their results showed that the first order reaction is the most effective mechanism for the first step of the biomass oxidation and coal combustion. It was found that the mixture of both, timber and solid waste, improve the devolatization of coal. Wood and coal interact significantly, with the reactivity being improved by the mixture.

In another study, Haseli et al. (2011) presented a detailed one-dimensional model for the combustion of a single particle of biomass and evaluated the accuracy of that model at different process conditions. The pyrolysis kinetic model used assumes that the raw biomass decomposes in light gases, tar (including heavy gases) and char through three concurrent reaction pathways. Reaction rates are determined by the Arrhenius equation.

Recently, Gubba et al. (2012) investigated through CFD modeling the co-combustion of pulverized coal and wheat straw in a 300 MW tangentially burning boiler for two thermal loads that have been studied experimentally. Wheat straw loads of 6% and 12% in mass flow were tested. The simulations showed agreement with experimental data.

The objective of present study is to numerically evaluate the influence of biomass particles size on the burning efficiency and on the emission of CO and CO_2, of an approximately 320 MW boiler that operates originally with pulverized coal. The CFD simulations were carried out using commercial software Ansys CFX 15.0 (Ansys Inc., 2011).

2. MATHEMATICAL MODEL

2.1 Mathematical formulation for coal combustion

The kinetic scheme for coal particles pyrolysis used in this work was proposed by Silva et al. (2010), assuming that coal is composed of raw coal, ash and moisture. The raw coal decomposes into volatile gases and residual carbon by two devolatization concurrent reactions, according to Ubayakar et al. (1976). The methane oxidation is modeled by two overall steps, the WD2 of Westbrok and Drier (1981). NOx formation is modeled through the NO-thermal, NO-prompt and NO-fuel mechanisms, according to the simplifications proposed by the methodology implemented in ANSYS - CFX (Ansys, Inc., 2011). Complementing this formulation, the drying of coal particles model proposed by Xianchun et al. (2009) was used. The kinetic parameters used in this reaction, namely the pre-exponential factor and the activation energy, are respectively $4.587x10^{12}$ s^{-1} and 78.995 kJ/kmol (Xianchun et al., 2009). For the residual char, the field char oxidation model (Ansys Inc., 2011) was adopted.

2.2 Mathematical formulation for biomass combustion

The kinetic scheme for the pyrolysis of biomass particles used in this work was proposed by Haseli et al. (2011) and assumes that the biomass is composed of raw biomass, ash and water. The raw biomass decomposes into light gases, tar (or heavy gases) and residual carbon through three parallel reactions. The model proposed by Bryden et al. (2002) for drying of wood biomass particles has been implemented. The chemical reaction rates are determined by Arrhenius model, accordingly to Ansys Inc., (2011). The kinetic constants were adopted from Di Blasi et al. (2001), accordingly to studies by Haseli et al. (2011), since they have good results for reactor at temperatures above 1100 K. Kinetic constants for particles drying were the same as used by Bryden et al. (2002). According to Grieco et al. (2011), the mass fraction of light gases, tar and residual carbon generated from the raw biomass decomposition are, respectively, 17%, 62% and 21%.

2.2.1 Homogeneous Reactions

The volatile components released during the pyrolysis process may react with other components and oxygen on the core and periphery of the particle. The mass fractions of the produced light gases depend on the heating conditions and the type of biomass. However, for engineering applications a constant composition is generally assumed. Di Blasi et al. (2001) propose the light gas composition to be 0.521, 0.156, 0.271, 0.021 and 0.031 for H_2O, CO, CO_2, CH_4 and H_2 respectively. For tar, an empirical simplification as $C_xH_yO_z$ is used. Bryden et al. (2003) analyzed the decomposition of tar and found that its main products are CO, CO_2, H_2O, H_2, CH_4, C_2H_6, C_2H_4, C_2H_2 and C_3H_6. They propose a chemical formulation represented by $C_{3.878}$ $H_{6.426}$ $O_{3.561}$, which has an O/C ratio of 0.918 and an H/C ratio of 1.657. Further information to describe the combustion rates of methane, hydrogen, carbon monoxide and tar can be obtained in Haseli et al. (2011). Gasification and combustion of the residual carbon are heterogeneous reactions. The residual carbon

gasification rates can also be obtained in Haseli et al. (2011). Gasification and combustion rate for residual carbon are determined through the Field Char Oxidation model adopted for char, incorporating the Arrhenius constants proposed by Hobbs et al. (1992).

2.3 Mass and species conservation

For a multicomponent fluid, scalar transport equations are solved for velocity, temperature and species mass fractions. The bulk motion of the fluid is modeled using single velocity, pressure, temperature and turbulence fields. The influence of the multiple components is felt only through property variation due to changes in composition. Each component has its own equation for mass conservation. After Favre-averaging the species conservation equation can be expressed in tensor notation as

$$\frac{\partial}{\partial x_j}\left(\overline{\rho}\tilde{U}_j\tilde{Y}_i\right)=\frac{\partial}{\partial x_j}\left(\left(\rho D_i+\frac{\mu_t}{Sc_t}\right)\frac{\partial\tilde{Y}_i}{\partial x_j}\right)+\overline{S}_i \tag{1}$$

where μ_t is the turbulent viscosity, Sc_t is the turbulent Schmidt number, $\overline{S}_i$ is the source term for component i which includes the effects of chemical reactions, D_i is the mass diffusivity, $\overline{\rho}$ is the average density, x is the spatial coordinate, $\tilde{U}_j$ is the vector of velocity and the mass fraction of component i was defined as $\tilde{Y}_i=\tilde{\rho}_i/\overline{\rho}$. Note that the sum of component mass fractions over all components is equal to one.

2.4 Momentum conservation

For the fluid flow the momentum conservation equations are given by:

$$\frac{\partial}{\partial x_j}\left(\overline{\rho}\tilde{U}_i\tilde{U}_j\right)=-\frac{\partial p^*}{\partial x_j}\delta_{ij}+\frac{\partial}{\partial x_j}\left(\mu_{eff}\frac{\partial\tilde{U}_i}{\partial x_j}\right)+\frac{\partial\tilde{U}}{\partial x_j\partial x_i}+\overline{S}_U \tag{2}$$

where $\mu_{eff}=\mu+\mu_t$, μ is the mixture dynamic molecular viscosity and $\mu_t=C_\mu\rho\,k^2/\varepsilon$ is the turbulent viscosity. The term $p^*=\overline{p}-(2/3)k$ is the modified pressure, C_μ = 0.09 is an empirical constant of the turbulence model, $\overline{p}$ is the time-averaged pressure of the gaseous mixture, and δ_{ij} is the Krönecker delta function. $\overline{S}_U$ is the source term, introduced to model the buoyancy and drag force due to the transportation particles, and other mathematical terms due to turbulence models. The Boussinesq model was used to represent the buoyancy force due to density variations. The k-ϖ model was used to model the turbulence on the flow (Wilcox, 1988).

2.5 Energy conservation

The energy equation can be written as

$$\frac{\partial}{\partial x_j}\left(\overline{\rho}\tilde{U}_j\tilde{h}\right)=\frac{\partial}{\partial x_j}\left(\kappa\frac{\partial\tilde{T}}{\partial x_j}+\sum_i^{Nc}\tilde{h}_i\left(\rho D_i+\frac{\mu_t}{Sc_t}\right)\frac{\partial\tilde{Y}_i}{\partial x_j}+c_p\frac{\mu_t}{Pr_t}\frac{\partial\tilde{T}}{\partial x_j}\right)+\overline{S}_{rad}+\overline{S}_{rea}+\overline{S}_T \tag{3}$$

where $\tilde{T}$, $\tilde{h}$ and c_p are the average temperature, enthalpy and specific heat of the mixture, $c_{p,i}$ and $\tilde{Y}_i$ are the specific heat and the average mass fraction of the i-th chemical species, κ is the thermal conductivity of the mixture, Pr_t is the turbulent Prandtl number, and $\overline{S}_{rad}$, $\overline{S}_{rea}$ and $\overline{S}_T$ represent the sources of thermal energy due to the radiative transfer, the chemical reactions and sink our source of energy. The term $\overline{S}_{rea}$ can be written as:

$$\overline{S}_{rea}=\sum_i\left[\frac{h_i^0}{\overline{MM}_i}+\int_{\tilde{T}_{ref,i}}^{\tilde{T}}c_{p,i}\,d\tilde{T}\right]\overline{R}_i \tag{4}$$

where h_i^0 and $\tilde{T}_{ref,i}$ are the formation enthalpy and the reference temperature of the i-th chemical species. To complete the model, the density of mixture can be obtained from the ideal gas state equation (Kuo, 1996; Turns, 2000), $\overline{\rho}=p\overline{MM}\left(\overline{\Re}\tilde{T}\right)^{-1}$, where p is the combustion chamber operational pressure, which is here set equal to 1 atm, and $\overline{MM}$ is the mixture molecular mass. The aforementioned equations are valid only in the turbulent core, where $\mu_t >> \mu$. Close to the wall, the conventional wall logarithmic law is used (Nikuradse, 1933).

For thermal radiation exchanges inside the combustion chamber, the Discrete Transfer Radiation Model (DTRM) was employed, considering isotropic scattering. The effect of the wavelength on gaseous phase was considered by WSGG model, using the coefficients obtained by Dorigon (2013). The WSGG model coefficients employed in this work were those for partial pressures of 0.1 atm and 0.2 atm for CO_2 and H_2O, respectively, being those values commonly considered for methane-air combustion, while the major species, N_2, is considered transparent to radiation. The radiative properties required for the particles are the absorption coefficients and scattering phase function, which depend on the particle concentration, size distribution, as well as effective complex refractive indices. However, optical properties of coal are not well characterized (Asotani et al., 2008). The particles were assumed as spherical and homogeneous. In this work, the heat transfer from gas mixture to particle considers that the particles are opaque bodies with emissivity equal to one (blackbodies), and the Hanz-Marshall correlation was used to model the heat transfer coupling between the gas mixture flow and the particles (Ansys Inc., 2004). In fact, heat transfer to the walls in coal combustion process is mainly due to radiation and the convective heat transfer has only a minor contribution (Xu et al., 2000).

2.6 The E-A (Eddy Breakup – Arrhenius) chemical reactions model

The reduced chemical reactions model employed in this work assumes finite rate reactions and a steady state turbulent process to volatiles combustion. In addition, it was considered that the combined pre-mixed and non-premixed oxidation occurs in two global chemical reaction steps, and involving only ten species: O_2, CH_4, H_2, H_2O, *Tar* ($C_{3.878}H_{6.426}O_{3.561}$), HCN, HCO, NOx, CO_2 e CO. Thus, one has the conservation equation for the *i*-th chemical species, given by Eq. (3), where the source term, S_i, considers the average volumetric rate of formation or destruction of the *i*-th chemical species in all chemical reactions. This term is computed from the summation of the volumetric rates of formation or destruction in all the k-th reaction where the *i*-th species is present, $\overline{R_{i,k}}$. Thus, $\overline{R_i} = \sum_k \overline{R_{i,k}}$. A combined Arrhenius-Magnussen model, the EBU-Arrhenius (Eaton et al., 1999), was used to obtain this rate.

3. MODEL VALIDATION

For verification purposes, the model developed in the present work was applied to the study case presented by Gu et al. (2010) which consists in burning coal in a simple geometry such as a tuyere (injector and burner of coal-oxidizer used in industrial furnaces), a device used to inject and burn coal in steel furnaces, Fig. 1. Comparing the results in Fig. 1a and 1-b, and 1c and 1-d, it can be observed that the two cases show similar velocity and temperature fields. The same modeling developed in this study was also applied to the case shown by Silva et al. (2010), obtaining similar results.

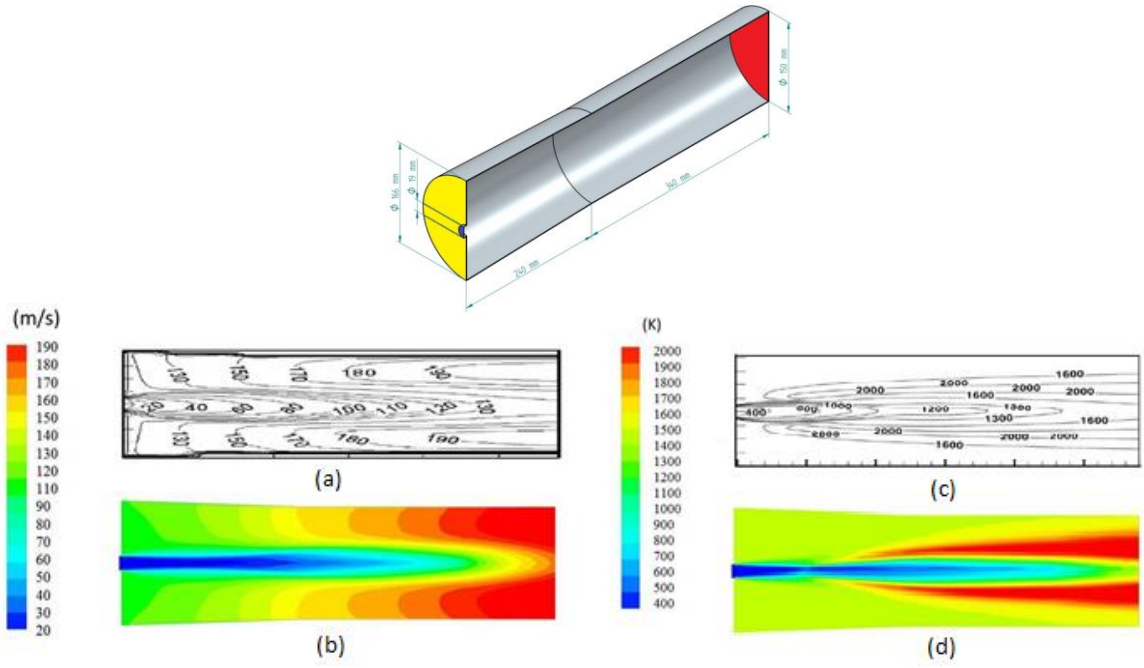

Figure 1: Temperature and velocity fields obtained from this modeling (b, d) and the results of Gu et al. (2010) (a, c).

4. PHYSICAL MODEL

The boiler in question is part of a 160 MW thermal power plant that uses pulverized coal. The combustion chamber has a square cross section of approximately 11 m and a height of approximately 53 m. The boiler operates through four tangential firing burners located on each corner of the combustion chamber with an inclination of 15° to the horizontal direction. Fig. 2 (c-d) shows the general arrangement of the burner and the horizontal boiler cross section.

5. GRID COMPUTING

The discretization within the boiler is performed with the implementation of tetrahedral volumes and prismatic volumes near the chamber walls. Figures 2-c and 2-d shows the geometry and the generated mesh in front view and in perspective. Grid independency tests were carried out among five grid systems with 0.9 million, 1.3 million, 1.5 million, 2.6 million, and 3.1 million elements. The mesh selected has around 1.5 million elements of different sizes, using mesh refinement in the reactive regions near the burners in a function of computational costs.

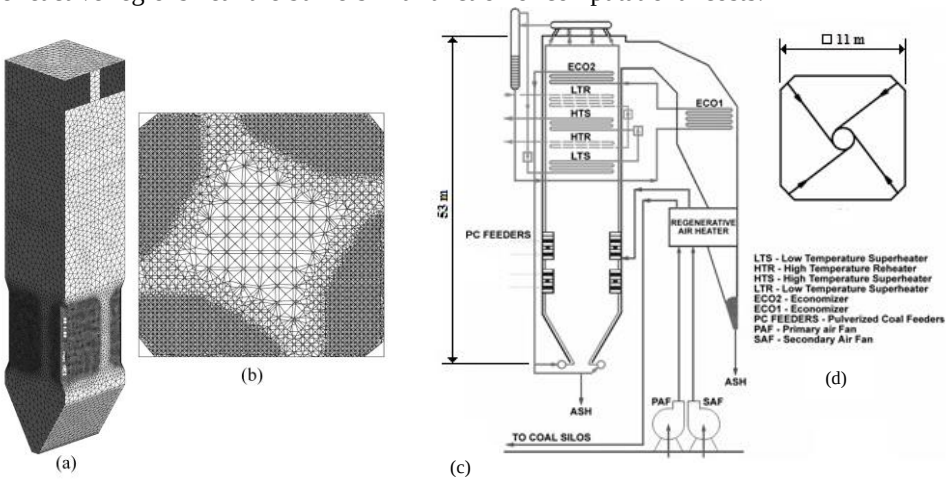

Figure 2. Mesh used in modeling: (a) perspective view and (b) cross section view (Silva et al., 2010); and geometry: (c) general arrangement of the boiler components and (d) horizontal boiler cross section (Silva et al., 2010).

6. BOUNDARY CONDITIONS

Boundary conditions and boiler design data were obtained from Silva et al. (2010), which evaluated the combustion of pure coal. The walls of the boiler, covered with steel tubes, were modeled as crude steel with a fixed temperature of 673 K, this being due to the saturation temperature of the water at the boiler working pressure. Thermal emissivity of the walls was assumed to be 0.9. Air flow, coal and biomass entering the combustion chamber by the burners were set as entry conditions: the mass flow rate of primary and secondary combustion air is 77.57 kg/s and 98.72 kg/s, respectively; pulverized coal and biomass mass flow rates are 47.50 kg/s and 0.84 kg/s, respectively. These values were obtained from Silva et al. (2010) via mass and energy balances (fuel and combustion air) on the boiler, considering a reduction of approximately 5% on coal flow for the inclusion of biomass, keeping the same thermal load provided for the boiler, about 320 MW. The lower heating value of coal and biomass used is 10301 kJ/kg and 14267.6 kJ/kg, respectively. The temperature of the primary air and coal with biomass is 542 K; the temperature of the secondary air is 600 K.

Pulverized coal particles size was modeled by probabilistic Rosin-Rammler distribution (Brown, 1995) and limited between 50 and 200 μm. Coal type CE 3100 and biomass of wood were used. The chemical composition and mass fraction of primary components of coal and wood due to the variation of moisture content is presented in Tab. 1.

Table 1. Chemical composition of coal CE 3100 and wood biomass.

Chemical species	**Coal CE 3100 concentration (%) (Silva et al., 2010)**		**Wood biomass concentration (%) (Mehrabian et al., 2012)**	
Primary components	**DRY BASES**	**WET BASES**	**DRY BASES**	**WET BASES**
Humidity	0	16.47	0	6
Raw coal	45.22	37.77	99.5	93.52
Ash	54.78	45.76	0.5	0.48
Mass fraction				
Humidity	0	16.47	0	6
Residual carbon	33.21	27.74	48.1	45.21
Ash	54.78	45.76	0.5	0.48
Oxigen	7.92	6.62	45.53	42.8
Hydrogen	2.34	1.95	5.77	5.42
Sulfur	1.14	0.95	-	-
Nitrogen	0.61	0.51	0.1	0.09

A pressure of -400 Pa was prescribed at the outlet of the modeled domain, based on the operating data. In order to evaluate the influence of the particle size on biomass co-firing, six case studies were considered and compared with a case of pure coal burning (base case) on the same operating conditions presented in Silva et al. (2010), although taking into account a model for drying the coal particles. The cases considered respectively the following sizes of biomass particles: Case 1 - 100 μm; Case 2 - 200 μm, Case 3 - 300 μm, Case 4 - 400 μm, Case 5 - 500 μm and Case 6 - 1000 μm.

7. RESULTS

The convergence criterion RMS - Root Mean Square was adopted, with values below $1x10^{-6}$ for all model variables. Fig. 3 shows temperature profiles on a vertical plane orthogonal to the boiler, for four of the six simulated cases, as well

as a temperature profile for the base case. Temperature profiles for cases 5 and 6 did not show large variations in relation to other cases and are not presented.

In Fig. 3 one can see that there was a general decrease in the temperatures values in the boiler when the co-combustion of coal with biomass is implemented, which, according Gubba et al. (2012), occurs due to the wood higher reactivity than the coal. Consequently, the devolatilization begins at a lower temperature, leading to a faster burning. Tab. 2 shows an average of the variables of interest in the domain output region for the six case studied, and compares these data with the burning of coal without biomass.

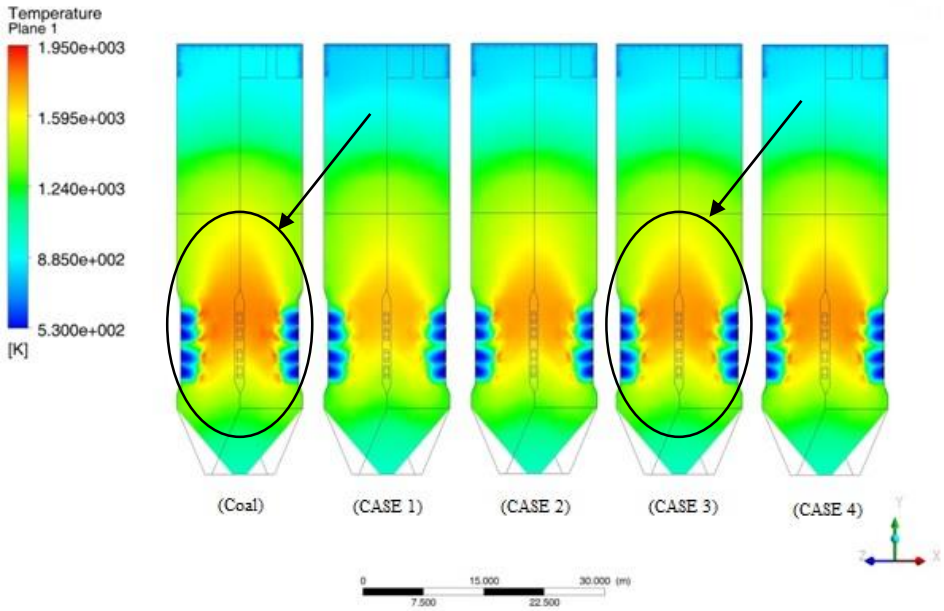

Figure 3. Temperature profile in a vertical transverse plane in the combustion chamber: (a) **base case**; (b) case 1 – 100 μm; (c) case 2 - 200 μm; (d) **case 3** - 300 μm and (e) case 4 - 400 μm.

Table 2. Average of variables in the boiler output region.

	Base Case	**Case 1 – 100 μm**	**Case 2 – 200 μm**	**Case 3 – 300 μm**	**Case 4 – 400 μm**	**Case 5 – 500 μm**	**Case 6 – 1000 μm**
CH_4 [ppm]	0.1039	0.0701	0.0682	0.0684	0.0684	0.0683	0.0681
CO [ppm]	0.7187	0.8890	0.7340	0.6990	0.6822	0.727	0.6516
Tar [ppm]	-	5.21×10^{-3}	1.08×10^{-4}	8.21×10^{-6}	2.89×10^{-6}	2.27×10^{-6}	1.11×10^{-6}
H_2 [ppm]	-	7.41×10^{-4}	1.52×10^{-4}	1.39×10^{-4}	1.41×10^{-4}	1.42×10^{-4}	1.44×10^{-4}
CO_2 [%]	20.95	20.84	20.73	20.72	20.71	20.71	20.71
H_2O [%]	9.14	8.89	8.88	8.89	8.89	8.89	8.89
N_2[%]	66.71	66.89	66.91	66.91	66.91	66.91	66.91
O_2[%]	3.15	3.35	3.43	3.44	3.44	3.45	3.45
Gas mass flow in the boiler output [kg/s]	204.03	200.35	200.29	200.30	200.30	200.29	200.29
Temperature [K]	875.1	822.3	839,4	845.2	848.0	849.5	853.0

Table 2 shows a slight reduction in CO_2 and H_2O emissions after the implementation of co-combustion in relation to the base case. The reduction in H_2O emissions is justified by the fact that the moisture content of coal is higher than that of biomass. Consequently the base case has a greater amount of water in the process and thus greater amount of H_2O after combustion. Biomass has a lower proportion of carbon than coal in its chemical composition, which may explain the reduction in CO_2 emissions. An increase in CO emissions in cases 1 and 2 was obtained, compared to the base case, implying that for biomass particle sizes less than 300 μm burning efficiency is decreased. From case 3 until case 6 it appears that CO emissions are lower than in the base case. It can be seen in Tab. 6 that CH_4 emissions decrease with inclusion of biomass. They also decrease with increasing the size of biomass particles until 200 μm, have a slight increase for biomass particle sizes between 200 and 400 μm and decrease in cases with particle sizes larger than 400 μm. With increasing particle size, tar and H_2 emissions decrease until case 3 (300 μm), increasing again from this. The increase in the amount of O_2 emitted for coal-biomass cases may be related to the fact that the biomass has a significant amount of oxygen in its own chemical composition.

Comparing the six cases, all variables show a small variation, except the temperature which gradually increases with increasing the size of biomass particles, with a considerable variation until case 3, and from this the average temperature at the output is no longer significant. It is observed that for coal-biomass co-firing, CO_2 formation rate is slightly smaller if compared to the base case, meaning that the burning efficiency is not impaired. Indeed, as shown in Tab. 2, there was a decrease of unburned fuel emissions.

Table 3 shows the average heat flux at the combustion chamber walls for the base case and the six cases studied. There is a decrease in heat flux t with biomass inclusion. Nevertheless, comparing only the heat flux for the cases with biomass, there is a significant increase with the increase in the biomass particles size.

Table 3. Heat flux trough the combustion chamber walls.

Heat flux trough chamber walls[kW/m²]	Base Case	Case 1-100 μm	Case 2-200μm	Case 3-300μm	Case 4-400μm	Case 5-500μm	Case 6-1000μm
	120.41	95.75	108.54	112.46	114.23	115.25	117.41

It appears that there is no wide variation among the presented cases. In order to better identify the differences between cases, Fig. 4 shows the temperature profile in the axial symmetry line for the base case (burning coal only) and the other six cases analyzed (coal-biomass). A temperature rise directly proportional to increase in size of the biomass particles is observed, the case 6 profile showing temperatures nearest to the base case ones.

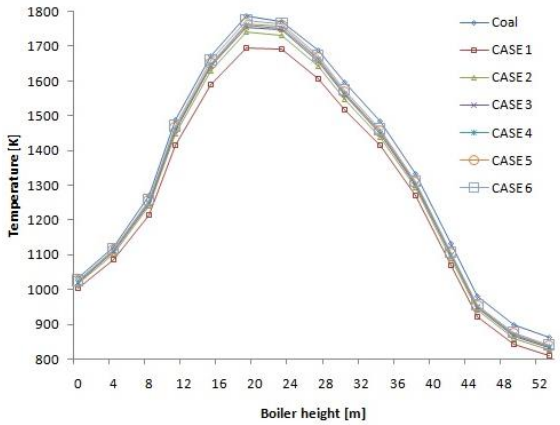

Figure 4. Temperature profiles in relation to boiler height in the axial symmetry line.

According to the analysis performed it seems possible the implementation of co-combustion of biomass as an alternative fuel for this boiler, which originally operates burning only coal. Case 3 shows a temperature profile and heat transfer rate at the walls of the boiler near the normal operating conditions. It may leads to a possible decrease in the steam generation because the heat transfer rate at the walls is, in fact, slightly lower than the basic case. Case 3 also presents lower emissions of CO, CO_2 and CH_4 compared to the base case, as can be seen in Tab. 2, and this shows an improvement in burning efficiency for coal-biomass mixture as a whole. Case 3 shows also smaller amount of H_2 emissions in relation to other cases evaluated.

Variations in properties for an increase in the biomass particle size in cases 4, 5 and 6 were evaluated and the results in terms of temperature field, mean temperature at outlet and heat transfer rate at the boiler walls, are increasingly closer to the boiler operating conditions when using only coal as fuel. Meanwhile the emission of unburned CO and CH_4 (but not H_2), decrease with increasing the size of biomass particles, which would justify the use of larger biomass particles. However, biomass particles with larger sizes (for the speed conditions of the primary air flow considered in this analysis) have more momentum and eventually collide with the walls of the equipment and fall to the bottom of boiler without having been burned completely.

8. CONCLUSIONS

At the end of this study, it can be conclude, from the thermodynamic point of view, that it is possible to implement the co-combustion process using coal and biomass in present equipment, within the boundary conditions considered in this analysis. The case 3, with sizes of biomass particles fixed at 300 μm, seems to .provide the best operational conditions.

9. ACKNOWLEDGEMENTS

The authors thank for the support of MCT/CNPq – National Research Council (Brazil).

10. REFERENCES

Ansys Inc, 2011. “User's guide - CFX Solver Theory”.

Brown, W. K., 1995. “Derivation of the Weibull distribution based on physical principles and its connection to the Rosin-Rammler and lognormal distributions”. *Journal of Applied Physics*, vol. 78, pp. 2758-2763.

Backreedy, R. I., Fletcher, L. M., Jones, J. M., Ma, L., Pourkashanian, M. and Williams, A., 2005. “Co-firing pulverized coal and biomass: a modeling approach”. Proceedings of the Combustion Institute, v. 30, p. 2955-2964.

Backreedy, R. I., Fletcher, L. M., Ma, L., Pourkashanian, M. and WILLIAMS, A., 2006. “Modeling pulverized coal combustion using a detailed coal combustion model”. *Combust. Sci. and Tech*., vol.178, p. 763-787.

Bryden, K. M., Ragland, K. W. and Rutland, C. J., 2002. “Modeling thermally thick pyrolysis of wood”. *Biomass and Bioenergy*, vol. 22, pp. 41-53.

Di Blasi, C. and Branca, C., 2001. “Kinetics of primary product formation from wood pyrolysis”. *Industrial and Engineering Chemistry Research*, vol. 40, p. 5547-5556.

Dong, C., Yang, Y., Yang, R. and Zhang, J., 2010. “Numerical modeling of the gasification based biomass co-firing in a 600 MW pulverized coal boiler”. *Applied Energy*, vol. 87, pp. 2834-2838.

Dorigon, L. J., Duciak, G., Brittes, R., Cassol, F., Galarça, M. and França F. H. R., 2013. "WSGG correlations based on HITEMP2010 for computation of thermal radiation in non-isothermal, non-homogeneous H_2O/CO_2 mixtures". *International Journal of Heat and Mass Transfer*, vol. 64, pp. 863-873.

Eaton, A. M., Smoot, L. D., Hill, S. C. and Eatough, C. N., 1999. "Components, formulations, solutions, evaluations, and application of comprehensive combustion models". *Progress in Energy and Comb. Sci.*, vol. 25, pp. 387-436.

Gil, M. V., Casal, D., Pevida, C., Pis, J. J. and Rubiera, F., 2010. "Thermal behavior and kinetics of coal/biomass blends during co-combustion". *Bioresource Technology*, vol. 101, pp. 5601-5608.

Grieco, E. and Baldi, G., 2011. "Analysis and modelling of wood pyrolysis". *Chemical Engineering Science*, v.66, p. 650-660.

Gu, M., Chen, G., Zhang, M., Huang, D.F., Chaubal, P. and Zhou, C.Q., 2010. "Three-Dimensional Simulation of the Pulverized Coal Combustion Inside Blast Furnace Tuyere". *Appl. Math. Modell*, vol. 34, pp. 3536-3546.

Gubba, S.R., Ingham, D.B., Larsen, K.J., Ma, L., Pourkashanian, M., Tan, H. Z., Williams, A. and Zhou, H., 2012. "Numerical modeling of the co-firing of pulverized coal and straw in a 300 MW tangentially fired boiler". *Fuel Processing Technology*, vol. 104, pp. 181–188.

Haseli, Y., Van Oijen, J. A. and De Goey, L. H. P., 2011. "A detailed one-dimensional model of combustion of a woody biomass particle". *Bioresource Technology*, vol. 102, pp. 9772-9782.

Hottel, H. C. and Sarofim, A. F. *Radiative Transfer*. McGraw-Hill, 1967.

Kuo, K. K. *Principles of combustion*. New York: John Wiley & Sons, 1996.

Lu, H., Robert, W., Peirce, G., Ripa, B. and Baxter, L. L., 2008. "Comprehensive study of biomass particle combustion". *Energy and Fuel*, vol. 22, pp. 2826-2839.

Ma, L., Jones, J. M., Pourkashanian, M. and Williams, A., 2007. "Modeling the combustion of pulverized biomass in an industrial combustion test furnace". *Fuel*, vol. 86, pp. 1959-1965.

Mehrabian, R., Zahirovic, S., Scharler, R., Obernberger, I., Kleditzsch, S., Wirtz, S., Scherer, V., Lu, H. and Baxter, L., 2012. "A CFD model for thermal conversion of thermally thick biomass particles". *Fuel Processing Technology*, vol. 95, pp. 96-108.

Nikuradse, J. *Strömusgsgesetze in Rauhen Rohren*. Forsch. Arb. Ing. – Ees.. VDI-Forsch 361, 1933.

Porteiro, J., Miguez, J. L., Granada, E. and MORAN, J. C., 2006. "Mathematical modeling of the combustion of a single wood particle". *Fuel Processing Technology*, vol. 87, p. 169-175.

Shafizadeh, F. and Chin, P. S., 1977. "Thermal deterioration of wood, Chemical Aspects". *ACS Symposium Series*, vol. 43, pp. 57-81, 1977.

Silva, C. V., Indrusiak, M. L. S. and Beskow, A. B., 2010. "CFD analysis of the pulverized coal combustion processes in a 160 MWe tangentially-fired-boiler of a thermal power plant". *Journal of the Brazilian Soc. Mechanical Sciences. & Eng.*, vol. XXXII, n. 4, p. 328-336.

Turns, S. T. *An introduction to combustion – Concepts and applications*. 2nd ed., New York, McGraw-Hill, 2000.

Wilcox, D. C., 1988. "Reassessment of the scale-determining equation for advenced turbulence models". *AIAA Journal*, vol. 26, p. 1299-1310.

Williams, A., Pourkashanian, M. anb Jones. J. M., 2001. "Combustion of pulverized coal and biomass". *Progress in Energy and Combustion Science*, vol. 27, pp. 587-610.

Westbrok, C.K. and Drier, C.K., 1981. "Simplified reaction mechanisms for the oxidation of hydrocarbon fuels in flames". *Combustion Science and Technology*, vol. 27, pp. 31-46.

Wurzenberger, J. C., Wallner, S., Raupenstrauch, H. and Khinast, J. G., 2002. "Thermal conversion of biomass: comprehensive reactor and particle modeling". *AIChE Journal*, vol. 48, p. 2398-2411.

Xianchun, L., Hui, S., Qi, W., Chatphol, M., Terry, W. and Jianglong, Y., 2009. "Experimental study on drying and moisture re-adsorption kinetics of an Indonesian low rank coal". *Journal of Environmental Sciences Supplement*, vol. 5, pp. 127-130.

Xu, M., Azevedo, J. L. T. and Carvalho, M. G., 2000. "Modeling of the combustion process and NOx emission in a utility boiler". *Fuel*, vol. 79, pp. 1611-1619.

Yang, Y. B., Sharifi, V. N., Swithenbank, J., Ma, L., Darvell, L. I., Jones, J. M., Pourkashanian, M. and Williams, A., 2008. "Combustion of a single particle biomass". *Energy and Fuels*, vol. 22, pp. 306-316. 2008.

Yin, C., Kaer, S. K., Rosendahl, L. and Hvid, S.L., 2010. "Co-firing straw with coal in a swirl-stablilized dual-feed burner: modeling and experimental validation". *Bioresource Technology*, vol. 101, pp. 4169-4178.

11. RESPONSIBILITY NOTICE

The author(s) is (are) the only responsible for the printed material included in this paper.